Published in final edited form as:
Inhal Toxicol. 2014 May ; 26(6): 361–369. doi:10.3109/08958378.2014.902147.

Neuroglobin mitigates mitochondrial impairments induced by acute inhalation of combustion smoke in the mouse brain

Falih Murat Gorgun, **Ming Zhuo**, **Shilpee Singh**, and **Ella W. Englander**
Department of Surgery, University of Texas Medical Branch Galveston, TX, USA

Abstract

Context—Acute inhalation of combustion smoke adversely affects brain homeostasis and energy metabolism. We previously showed that overexpressed neuroglobin (neuron specific globin protein) attenuates the formation of smoke inhalation-induced oxidative DNA damage, in vivo, in the mouse brain, while others reported protection by neuroglobin in diverse models of brain injury, mainly involving oxidative stress and hypoxic/ischemic insults.

Objective—To determine to what extent elevated neuroglobin ameliorates post smoke-inhalation brain bioenergetics and homeostasis in neuroglobin overexpressing transgenic mouse.

Methods—Smoke inhalation induced changes in bioenergetics were measured in the wild type and neuroglobin transgene mouse brain. Modulations of mitochondrial respiration were analyzed using the Seahorse XF24 flux analyzer and changes in cytoplasmic energy metabolism were assessed by measuring enzymatic activities and lactate in the course of post smoke recovery.

Results—Cortical mitochondria from neuroglobin transgene, better maintained ATP synthesis-linked oxygen consumption and unlike wild type mitochondria did not increase futile oxygen consumption feeding the proton leak, reflecting lesser smoke-induced mitochondrial compromise. Measurements revealed lesser reduction of mitochondrial ATP content and lesser compensatory increases in cytosolic energy metabolism, involving pyruvate kinase and lactate dehydrogenase activities as well as cytosolic lactate levels. Additionally, induction of c-Fos, the early response gene and key neuronal stress sensor, was attenuated in neuroglobin transgene compared to wild type brain after smoke.

Conclusion—Considered together, these differences reflect lesser perturbations produced by acute inhalation of combustion smoke in the neuroglobin overexpressing mouse, suggesting that neuroglobin mitigates mitochondrial dysfunction and neurotoxicity and raises the threshold of smoke inhalation-induced brain injury.

Keywords

bioenergetics; brain; mitochondria; neuroglobin; oxygen consumption; smoke inhalation

Corresponding author: Ella W. Englander, PhD, Department of Surgery, University of Texas Medical Branch, 301 University Boulevard, Galveston, Texas 77555, Phone: (409) 772-8197, elenglander@utmb.edu.

DECLARATION OF INTEREST
The authors declare that there are no conflicts of interest.

INTRODUCTION

Neuroglobin (Ngb), a member of the oxygen binding family of globin proteins, is expressed in brain region-specific manner in neuronal cells (Burmester et al., 2000; Hundahl et al., 2008; Hundahl et al., 2010). Although Ngb is evolutionarily conserved and has ancient evolutionary origins (Droge et al., 2012), its actual mode of action is not well understood (Burmester, Hankeln, 2009). To date, reports have implicated Ngb in brain protection in different injury settings via diverse mechanisms, which include augmentation of mitochondrial homeostasis, oxygen binding and sensing, neutralization of reactive oxygen and nitrogen species, redox cycling (Sun et al., 2003; Khan et al., 2006; Kiger et al., 2011; Li et al., 2011; Brittain, Skommer, 2012), brain region- and neuron type-specific adaptive regulatory functions (Hundahl et al., 2008; Hundahl et al., 2012) and serving as an oxidative stress sensor, which is recruited to lipid rafts to suppress activation of G-proteins in favor of neuronal survival (Watanabe, Wakasugi, 2008; Watanabe et al., 2012).

We recently produced a genetically modified mouse strain with neuron-specific, physiologically relevant overexpression of Ngb (Ngb-tg) under the control of synapsin 1 promoter (Lee et al., 2011). Because previously Ngb was found neuroprotective in several settings of brain injury, we sought to elucidate potential roles of elevated Ngb in a setting of acute inhalation of combustion smoke. We had developed the awake rodent model of smoke inhalation (Lee et al., 2005; Lee et al., 2009; Lee et al., 2010) to facilitate investigation of mechanisms, which underlie neurological deficits that tend to develop in survivors of acute inhalation of combustion smoke (Hartzell, 1996; Rossi et al., 1996; Stefanidou et al., 2008). We investigated the effects of elevated neuronal Ngb, in vitro, in a setting of nitric oxide challenge (Singh et al., 2013) and in vivo, in a model of acute inhalation of smoke (Lee et al., 2011). We found that in vivo, elevated Ngb exerts protection by lessening smoke inhalation induced formation of oxidative DNA damage in the mouse brain (Lee et al., 2011). Because the injurious components of combustion smoke, including carbon monoxide, toxic gases, volatile organic compounds, particulates and hypoxic environment, combine to impede oxygenation, disrupt energy metabolism, and initiate the progression of brain injury, the present study, is focused on the status of brain bioenergetics. Using the Seahorse Bioscience metabolite flux analyzer, key parameters of mitochondrial function were assessed. Specifically, we aimed to determine which parameters of mitochondrial respiration might be better preserved after smoke exposure in the presence of elevated neuroglobin, and thereby mitigate disruption of brain energy metabolism, curtail resultant oxidative stress and initiation of smoke-induced brain injury.

MATERIALS AND METHODS

Mouse model of smoke inhalation

We have previously developed combustion smoke-inhalation model for the awake rodent (Lee et al., 2005; Chen et al., 2007; Lee et al., 2009; Lee et al., 2010; Lee et al., 2011). Male CB57BL/6 mice (25–30 gram) wild type and transgenic (Ngb-tg), with neuron specific overexpression of neuroglobin under the control of rat synapsin 1 promoter were used (Lee et al., 2011). Ngb-tg homozygotes were utilized in all experiments in parallel with the wild type strain. Briefly, awake mice were exposed to smoke generated by smoldering wood

shavings (1.3 gram/minute) in a smoke generating container connected to a 20-liter transparent exposure chamber. Mice were exposed to smoke for 60 minutes with venting to ambient air for 10–20 seconds at approximately 10 minutes intervals. Following exposure mice were let recover for 0, 1, 2, 6 or 24 hours before sacrifice and tissue collection for the different types of assays; survival rate was > 95%. Mice handled identically, except for the omission of smoke served as sham controls. All procedures were conducted in accordance with mandated standards of humane care and were approved by the Institutional Animal Care and Use Committee.

Reagents

Chemicals were from Sigma, unless stated otherwise: Sodium pyruvate (P5280), L-(−) Malic acid (M6413), L-Glutamic acid monosodium salt monohydrate (49621), Sodium succinate dibasic hexahydrate (S2378), oligomycin (O4876), carbonyl cyanide *4*-trifluoromethoxyphenylhydrazone (FCCP) (C2920), antimycin A (A8674), ADP (A2754). Antibodies: heme oxygenase-1 monoclonal (sc-136960, Santa Cruz), VDAC1 (sc-8828, Santa Cruz), neuroglobin (RD181043050, BioVendor).

Mitochondrial isolation

Crude mitochondria were prepared based on the method of Anderson and Sims (Anderson, Sims, 2000) modified as in Fisar et al., (Fisar et al., 2010) and as we previously described (Lee et al., 2010). All procedures were done on ice; the different samples were handled in parallel to ensure uniform length of time between tissue collection and Seahorse respiratory measurements (3.5 hours) to avoid technical differences and minimize mitochondria uncoupling associated with processing. Cortices were dissected out, finely cut on ice and homogenized by four strokes of loose fitting pestle in ice-cold mannitol-sucrose-EDTA (MSE) mitochondria isolation buffer (0.225 M mannitol, 0.075 M sucrose, 0.1 mM EDTA pH 7.4, fatty acid free BSA 5 mg/ml), followed by 15 strokes of tight fitting pestle and centrifuged (Eppendorf refrigerated microcentrifuge 5415R) for 10 minutes at 2200 g to pellet cell nuclei. Supernatants were collected and centrifuged for 12 minutes at 15,000 g to obtain crude mitochondrial pellets. Pellets were washed twice with 0.25 M sucrose, spun at 6000 g, re-suspended in 60 μl MSE buffer and protein concentrations were determined (Bradford assay reagent, Biorad). We use crude mitochondrial preparations as further purification by Percoll gradient centrifugation results in markedly reduced mitochondrial yields, which are insufficient for assaying respiratory parameters of mitochondria from a single mouse cortex (Sims, Blass, 1986; Sims, Anderson, 2008; Hroudova, Fisar, 2012).

For Seahorse XF24 analyses, aliquots of mitochondrial suspension (6 μg) were gently mixed into precooled tubes containing 50 μl of mitochondrial assay solution-MAS (70 mM sucrose, 220 mM mannitol, 10 mM KH_2PO_4, 5 mM $MgCl_2$, 2 mM HEPES, 1.0 mM EGTA and 0.2% (w/v) fatty acid free BSA, pH 7.2) (Rogers et al., 2011) and transferred into coated (poly-L-lysine 50 μg/ml) wells of Seahorse XF24 plate; plates were spun in Eppendorf 5810R centrifuge (A-2-DWP-AT swinging rotor) at 2000 g for 25 minutes/4°C to create uniformly distributed mitochondrial layer (Flynn et al., 2011). Following centrifugation, wells were supplemented with additional MAS (625 μl), swiftly inspected at 20X magnification to

verify adherence of mitochondria to the well bottom and pre-warmed at 37°C for 8 minutes prior to XF24 analyses.

Seahorse XF24 analyses

Mitochondrial respiration was measured using the Seahorse XF24 flux analyzer (Seahorse Bioscience, North Billerica, MA). All procedures were according to manufacturer's recommendations (Gerencser et al., 2009; Rogers et al., 2011) and as we described (Singh, Englander, 2012; Singh et al., 2013). Measurements were done using freshly isolated crude mitochondria processed as detailed above. Assay protocol was implemented by the XF24 Reader software Version 1.7. Mitochondrial substrates (succinate, malate, pyruvate and glutamate) and ADP were given through the first port to initiate state 3 respiration (5 mM-final in well concentration). This was followed by sequential additions of oligomycin (3 μg/ml) to inhibit complex V and thereby ATP synthesis, the uncoupler FCCP (3 μM) and antimycin A (5.4 μM) to block complex lll; these concentrations were determined and optimized by prior titration under our experimental conditions. Three measurements at 5-minute intervals were obtained for each segment of the assay. Modulations of activities by mitochondrial effectors translate into changes in oxygen consumption rates (OCR), enabling computation of relative changes induced by a given treatment, versus parallel changes measured in non-treated controls (Abe et al., 2010; Brand, Nicholls, 2011; Dranka et al., 2011), respectively, in the transgene and wild type brain.

Mitochondrial immunofluorescent staining

Aliquots (10 μl) of mitochondrial suspensions (prepared as above) were added to MAS (190 μl), mixed gently prior to placing 50 μl aliquots on poly-D-lysine (50 μg/ml) coated coverslips and incubated 60 minutes in a humidified chamber at 25°C. Coverslips were fixed with 3% paraformaldehyde for 20 minutes at 37°C. Permeabilization was with 0.2% Triton-X-100 for 10 minutes followed by washing with 1% BSA and blocking with 3% BSA + 1% donkey serum for 30 minutes. Incubation with primary antibodies was overnight at 1:300 dilution of anti-cytochrome c monoclonal antibody (MSA06, MitoSciences) and 1:400 dilution of synapsin 1 (sc-8295, Santa Cruz) in 1% BSA followed by a 2-hour incubation with donkey anti-mouse alexa 488 and donkey anti-goat alexa 546 fluor 1:800 secondary antibodies. Typically, a field with 2000–2500 particles was examined using the IX71 Olympus fluorescence microscope equipped with a QIC-F-M-12-C cooled mono 12 BIT digital camera (QImaging, Surrey, BC, Canada) with 40X objective. Mitochondrial and synaptosomal particles were quantified using the NIH ImageJ software.

Mitochondrial ATP content measurement

Mitochondrial ATP content was determined using the ATP Bioluminescence Assay Kit HS II (Roche Molecular Biochemicals, Indianapolis, IN). Freshly isolated mitochondrial pellets were extracted according to manufacturer's instructions with some modifications (Singh, Englander, 2012), sonicated (Sonic Dismembrator Model 100, Fisher Scientific) and centrifuged at 16000 g for 8 minutes at 4°C. The supernatant was collected, diluted with Tris-acetate buffer pH 7.6 and 50 μl aliquots were transferred to black microtiter plates and mixed with equal volume of the luciferase reagent (ATP Bioluminescence Assay Kit HS lI). Measurements of luminescence were at 5-second integration time (TECAN Genios plate

reader). ATP amounts were calculated from log-log graphs generated for ATP standard using Magellan software and normalized to mitochondrial protein.

Measurements of cytosolic enzymes and lactate concentration

Cytosolic enzymatic activities were determined spectrophotometrically as described (Bergmeyer et al., 1974). Briefly, the pyruvate kinase reaction was assembled with 0.1 M Tris-HCl pH 7.6, 17 mM phosphoenolpyruvate, 1.3 mM NADH, 100 mM MgSO4, 44 mM ADP and freshly dissolved lactate dehydrogenase (10 units). After 5-minute preincubation at 37°C, the reaction was initiated by the addition of 40 μg of cytosolic fraction and decrease in absorbance was measured at 340 nm; activity was calculated using an extinction coefficient of 6.22 mM 1 cm 1. Measurement of lactate dehydrogenase (LDH) activity was in a reaction containing 0.1 M Tris-HCl pH 7.0, 10 mM sodium pyruvate, and 0.3 mM NADH (Renner et al., 2003). Reaction mix was preincubated (5 min, 30°C) prior to the addition of cytosolic fraction (40 μg); optical density was measured at 340 nm for 2 minutes at 30-second intervals. LDH activity was calculated using an extinction coefficient of 6.22 mM 1 cm 1. Cytoplasmic lactate content was measured using the L-lactate Kit l #1200014002 (Eton Bioscience) according to manufacturer's instructions.

Real Time qPCR

Total RNA was isolated using RNeasy plus mini kit (Qiagen) and RNA was reverse transcribed using iScript RT supermix (Biorad) which contains random and oligo dT primers. Real-time PCR analyses were done using the CFX96 Real-Time System (Biorad). PCR reactions were assembled with SSO FAST Evagreen supermix (Biorad) and PCR amplification program was: 95°C 2 minutes, 40 cycles of 95°C 5 seconds, 55°C 15 seconds with plate reading and subsequent melting curve analysis using 18S ribosomal RNA gene as reference gene. Data represent the mean of 5 independent experiments. The relative amount of target gene was calculated as described (Schmittgen, Livak, 2008) using the formula: $-\Delta\Delta Ct$ = [(CT gene of interest-CT internal control) sample-(CT gene of interest-CT internal control) control]. For c-Fos expression analysis the primers were 5′-gggacagcctttcctactacc-3′ and 5′-gatctgcgcaaaagtcctgt-3′ (NM_010234) and for 18S 5′-gtaacccgttgaaccccatt-3′ and 5′-ccatccaatcggtagtagcg-3′ (NR_003278).

Statistical analyses

Group measures are presented as means ± SEM. Two-tailed Student's t-test was used for two groups analyses, and one way analysis of variance (ANOVA) followed by Bonferroni post hoc test was used when more than two groups were compared; *p*-value of less than 0.05 was considered significant. For Seahorse analyses, mitochondria from at least six mice per treatment groups were assayed; mice were obtained from three or more independent sets of smoke exposure experiments.

RESULTS

Characterization of crude mitochondrial preparations

Crude mitochondrial preparations were examined by immunofluorescent staining and Western blotting analyses. The synaptosomal component was estimated by Western and

immunofluorescent (IF) detection of the synaptosomal protein, synapsin 1. For IF, mitochondrial suspensions were spread on coverslips and incubated for 60 minutes to ensure adherence prior to fixation and probing with anti-cytochrome c and anti-synapsin 1 antibodies (Fig. 1A). About 2000 particles per coverslip were screened. Analysis revealed approximate ratio of 1:2 between synaptosomal (syn-1 positive, red) and cyto c positive (green) particles (Fig. 1B). There were no differences in particles ratios between the wild type and Ngb-tg preparations (wild type images are shown). As expected, Western blotting analyses of mitochondrial preparations (Fig. 1C) revealed in addition to the mitochondrial proteins, cytochrome c and VDAC1, significant levels of the synaptosomal protein, synapsin 1. While there were no measurable differences in levels of these proteins between the wild type and Ngb-tg preparations, in the case of Ngb-tg, Westerns were positive also for the Ngb protein (Fig. 1C), possibly associated with mitochondria captured in synaptosomes. Detection of overexpressed Ngb protein in our mitochondrial preparations is consistent with the previously demonstrated close association of the Ngb protein with these organelles (Lechauve et al., 2012; Yu et al., 2012). However, considering the brain region-specific localization and low expression (Hundahl et al., 2008; Hundahl et al., 2010), endogenous Ngb protein is expected to be below Western detection level in cortical synaptosomes from the wild type mouse.

Acute inhalation of combustion smoke affects differentially mitochondrial respiration in the wild type and Ngb-tg brain

Mitochondria from cortices of wild type and Ngb-tg sham-control mice and mice sacrificed immediately or one hour after acute exposure to combustion smoke were analyzed. Respiratory parameters were assessed using the Seahorse analyzer 24-well plate format. Uniform distribution and adherence of mitochondria to wells were visually verified prior to measurements (Fig. 1D, 20x). Seahorse XF24 analyzer executes real-time measurements of changes in OCR in response to sequential additions of mitochondrial effectors, supporting parallel comparisons between controls and different treatment groups. Typically, mitochondria from each six-mouse set representing the six treatment groups monitored in this study were analyzed in the same Seahorse plate. Mitochondrial preparations from individual mouse cortices were aliquoted into 3–4 wells and their respective average OCR readings were generated by the Seahorse software. Graphs (Fig. 2A) represent mean OCR values calculated from average readings of six mice for each treatment group, which have been obtained in at least three independent sets of smoke experiments. In the first segment of XF24 measurements, the baseline OCR for isolated mitochondria was measured, followed by recordings of ATP synthesis linked OCR (state 3 respiration) which was initiated by the addition of ADP. Subsequent addition of oligomycin, an inhibitor of complex V (which blocks ATP synthase) revealed the portion of OCR which is uncoupled from ATP synthesis and reflects the extent of consumed oxygen that feeds the proton leak, which is inversely proportional to membrane integrity. The addition of FCCP, an ionophore that carries protons across the inner membrane independently of ATP synthesis, reveals cell type specific mitochondrial capacity for substrate oxidation. The extent of non-mitochondrial OCR, which was measured after subsequent addition of antimycin A, was at ~10% of state 3 respiration, plausibly reflecting molecular oxygen consumed by plasma membrane bound oxidases. This non-mitochondrial portion of OCR was subtracted from all calculations

(Brand, Nicholls, 2011). The respective contributions of the different oxygen consuming processes (bioenergetic profile), i.e., ATP synthesis linked respiration (state 3), proton leak and FCCP response, were compared among mitochondrial preparations from sham-controls and smoke exposed mouse cortices from wild type and Ngb-tg mice (Fig. 2A). At the immediate, 0-hour recovery time neither the wild type nor Ngb-tg OCR values were significantly changed by acute exposure to smoke. In contrast, at the one hour recovery following smoke exposure, ATP synthesis linked respiration (state 3) measured in wild type mitochondria was 40% lower compared to sham controls, while OCR for Ngb-tg mitochondria was only ~15% lower than the respective sham-controls at that recovery time (Fig. 2B). In addition, at the one hour recovery time post smoke, OCR feeding the proton leak increased by more than 25% in wild type mitochondria, while no significant change in OCR associated with proton leak was detected in Ngb-tg mitochondria (Fig. 2B). OCR induced by subsequent addition of FCCP was ~25% lower in wild type mitochondria when compared to sham controls, while the reduction in OCR detected in Ngb-tg mitochondria was not statistically significant, suggestive of a lesser compromise of substrate oxidation processes by exposure to smoke. Taken together, OCR measurements revealed lesser impairments of mitochondrial status by smoke in the Ngb-tg compared to wild type brains.

Because smoke exposures differentially affected mitochondrial respiratory parameters (Fig 2), we asked whether these differences might be accompanied by changes in the mitochondrial ATP content. ATP content measurements showed a reduction of approximately 50% and 35%, respectively, in the wild type and Ngb-tg mitochondria, at both the 0- and 1-hour recovery times post smoke (Fig. 3). This suggests that mitochondrial ATP content after smoke might reflect not only differences in ATP synthesis rates (Fig. 2), but also differential ATP export rates and turnover in extramitochondrial compartments (Atlante et al., 2003; Atlante et al., 2011) in response to changing cellular energy metabolism under compromised conditions.

Acute smoke inhalation differentially modulates cytosolic pyruvate kinase (PK), lactate dehydrogenase (LDH) and lactic acid levels in the wild type and Ngb-tg brain

To assess whether in view of differential impact on brain mitochondria, cytosolic energy metabolism might be also differentially affected by acute smoke inhalation in Ngb-tg and the wild type brain, cytosolic pyruvate kinase and lactate deydrogenase activities as well as lactic acid levels were measured (Fig. 4). Smoke exposures caused substantial increases in cytosolic PK and LDH activities. Increases ranging from 20% to 90% were observed, peaking at the 2-hour recovery time point after smoke exposure. PK and LDH activities remained elevated to a greater extent at 6- and 24-hour recovery in the wild type compared to Ngb-tg brain, with a similar pattern of alterations observed for cytoplasmic lactate levels. Interestingly, at the 24-hour recovery time levels of PK, LDH and lactate returned to near normal in Ngb-tg, but remained significantly elevated in the wild type brain.

c-Fos gene expression and heme oxygenase-1 protein levels are induced by smoke inhalation to a lesser extent in Ngb-tg compared to the wild type mouse

Because c-Fos is a key stress sensor in the nervous system (Cui, Liu, 2001), we asked whether the magnitude of c-Fos induction might inform on differences in oxidative stress

levels in the wild type and Ngb-tg brains challenged by acute exposure to combustion smoke. Real-Time qPCR analyses revealed a nearly 300% induction of c-Fos mRNA in the wild type brain, versus only 180% in Ngb-tg at the 1-hour recovery time, and approximately 250%- and 120% at 24-hour recovery post smoke for wild type and Ngb-tg, respectively (Fig. 5A). The phase ll, stress response enzyme, heme oxygenase-1 (HO-1), was also differentially modulated. A nearly 4-fold induction in cortical HO-1 protein level was observed by 2-hours post smoke in the wild type cortex, while HO-1 levels were elevated to a lesser extent in Ngb-tg, with shorter duration and return to normal already by 6-hours post smoke (Fig. 5B).

DISCUSSION

Inhalation of combustion smoke produces a complex insult involving toxic gases, volatile organic compounds, particulate matter and hypoxia (Lee et al., 2010; Chan et al., 2013; Loane et al., 2013), which combine to disrupt oxygenation, impair mitochondrial energy metabolism, induce ROS and increase oxidative stress, severely impacting brain bioenergetics and function. Accordingly, brain manifestations of acute exposure to combustion smoke span a broad range of adversely affected targets (Lee et al., 2005; Lee et al., 2009; Zou et al., 2009; Lee et al., 2010; Lee et al., 2011; Zou et al., 2013) and we sought to identify those targets, which are protected by neuroglobin in this setting. To this end, we first produced a transgenic mouse with neuron-specific overexpression of Ngb and demonstrated that Ngb protects primary neurons by raising the threshold of nitric oxide mediated neuronal injury (Singh et al., 2013) and that in vivo, elevated Ngb attenuates the formation of smoke-induced oxidative DNA damage in the mouse brain (Lee et al., 2011). Because the formation of oxidative DNA damage is thought to be driven primarily by excessive ROS, which is incidental to perturbed mitochondrial energy production, the objective of the present study was to compare the status of key parameters of mitochondrial respiration in the wild type and Ngb-tg mice after acute exposure to combustion smoke. We found that perturbations of brain bioenergetics by smoke were measurably curtailed in Ngb overexpressing compared to the wild type mouse strain. Specifically, mitochondrial oxygen consumption, devoted to ATP synthesis, was reduced by smoke exposure to a greater extent in the wild type brain, where it was also accompanied by a significant increase in futile oxygen consumption feeding the proton leak. In contrast, increases in proton leakage were not observed in Ngb-tg mitochondria after smoke, suggesting lesser smoke induced uncoupling in Ngb-tg when compared to the wild type mitochondria. Likewise, the diminution of mitochondrial ATP content after smoke was greater in the wild type when compared to Ngb-tg brain. Moreover, in the wild type brain, key cytosolic enzymes involved in brain energy metabolism, pyruvate kinase and lactate dehydrogenase were elevated to a greater extent, most likely reflecting a more robust compensatory response needed to satisfy energy demands, which could not be met by the wild type mitochondria, which have been compromised by exposure to combustion smoke. Accordingly, brain levels of lactic acid after smoke inhalation increased more in the wild type compared to Ngb-tg brain. Because Ngb is localized primarily to the cytosol (Hankeln et al., 2004; Singh et al., 2013), it cannot be precluded that elevated Ngb can affect pyruvate kinase and lactate dehydrogenase activities by mechanism not yet identified. However, it is likely that attenuated induction of

cytosolic enzymes and lactate levels in the Ngb-tg brain reflects on better preserved mitochondrial respiration and subsequently a relatively limited need for compensatory metabolic shift away from mitochondrial energy production after smoke. Interestingly, in a recent study, elevation of brain lactate levels has been linked with chronological- and mitochondrial DNA mutator-driven aging phenotypes (Ross et al., 2010). Thus, elevated brain lactate coincides with mitochondrial impairments and brain pathologies consistent with the brain aging process and other compromising conditions associated with declining brain function. Since elevated lactic acid and resultant acidosis might drive neuronal injury also via inflammatory processes (Edye et al., 2013), the possibility that overexpressed Ngb mitigates the magnitude of the shift to glycolytic metabolism and subsequently also the onset of acidosis, might account in part for its neuroprotective effects observed in this setting. Intriguingly, in gills of zebra fish, several globin proteins, including Ngb are upregulated as a part of adaptive response to environmental acidosis (Tiedke et al., 2013).

Interestingly, the appreciably greater modulations of energy metabolism indicators in the wild type brain were also accompanied by markedly stronger induction of the central neuronal stress sensor, the c-Fos gene (Shimokawa et al., 2005; Kovacs, 2008) and the phase ll antioxidant response enzyme, heme oxygenase- 1 (HO-1) (Ghosh et al., 2011) in the wild type when compared to Ngb-tg brain. Notably, a link between Ngb levels and regulation of the c-Fos gene was reported in an earlier study where exacerbated c-Fos response to hypoxia was observed in Ngb knockout mouse, suggesting that Ngb deficiency might sensitize the brain to hypoxic brain injury (Hundahl et al., 2011). Taken together, our new findings are consistent with the scope of previously observed neuroprotective effects of elevated Ngb, as in the majority of reported injury models, the proposed modes of neuroprotection by Ngb have been linked with improved sustenance of mitochondrial function (Yu et al., 2013). The proposed mechanisms by which Ngb might ameliorate mitochondrial function in support of neuronal survival, include involvement in augmentation of respiratory chain function (Kiger et al., 2011; Lechauve et al., 2012), interactions with cytochrome c (Fago et al., 2006; Raychaudhuri et al., 2010; Fiocchetti et al., 2013), preservation of respiratory complex lV activity by sequestration of excessive nitric oxide (Brunori et al., 2005; Singh et al., 2013) as well as neutralization of free radicals (Herold et al., 2004; Fordel et al., 2007; Li et al., 2011).

By monitoring key indicators of brain energy metabolism after acute exposure to combustion smoke, we identified specific targets, which were differentially affected in the presence and absence of elevated Ngb. Importantly, in Ngb-tg, compared to wild type cortical mitochondria, productive oxygen consumption linked with ATP synthesis was less affected and no increases in the proton leak were observed, reflecting on better sustained respiratory complexes and better retained membrane integrity in Ngb-tg mitochondria after smoke exposure. The observed Ngb involvement in amelioration of mitochondrial function provides new insights into mechanisms underlying better sustenance of Ngb-tg mitochondria in the setting of smoke exposure. Because ROS generation is downstream of impaired mitochondrial respiration, and oxidative DNA damage is downstream of excessive ROS, it is plausible that the observed attenuation of smoke-induced DNA damage formation in the Ngb-tg brain (Lee et al., 2011) resulted, at least in part, from prevention of mitochondrial dysfunction and diminution of ROS.

CONCLUSIONS

In view of the well-recognized central role of mitochondria in brain health and because impaired mitochondrial function has been implicated in the etiology of different neurodegenerative diseases (Wallace, 2013; Zsurka, Kunz, 2013), the possibility that neuroglobin might protect neurons by augmenting mitochondrial function under compromising conditions as previously suggested and further corroborated in this current report, has broad implications for interventional strategies for protection of neurons via neuroglobin-mediated preservation of mitochondrial fitness.

Acknowledgments

This work was supported by grants from Shriners Hospitals for Children (8670) and the National Institutes of Health (ES014613 and NS034994) to EWE. We thank Eileen Figueroa and Steve Schuenke for help with manuscript preparation.

References

Abe Y, Sakairi T, Kajiyama H, et al. Bioenergetic characterization of mouse podocytes. Am J Physiol Cell Physiol. 2010; 299:C464–76. [PubMed: 20445170]

Anderson MF, Sims NR. Improved recovery of highly enriched mitochondrial fractions from small brain tissue samples. Brain Res Brain Res Protoc. 2000; 5:95–101. [PubMed: 10719270]

Atlante A, de Bari L, Bobba A, et al. Cytochrome c, released from cerebellar granule cells undergoing apoptosis or excytotoxic death, can generate protonmotive force and drive ATP synthesis in isolated mitochondria. J Neurochem. 2003; 86:591–604. [PubMed: 12859673]

Atlante A, Seccia TM, Marra E, et al. The rate of ATP export in the extramitochondrial phase via the adenine nucleotide translocator changes in aging in mitochondria isolated from heart left ventricle of either normotensive or spontaneously hypertensive rats. Mech Ageing Dev. 2011; 132:488–95. [PubMed: 21855562]

Bergmeyer, HU.; Gawehn, K.; Grassl, M. Enzymes as biochemical reagents. In: Bergmeyer, HU., editor. Methods of Enzymatic Analysis. New York: Academic Press; 1974. p. 509-10.

Brand MD, Nicholls DG. Assessing mitochondrial dysfunction in cells. Biochem J. 2011; 435:297–312. [PubMed: 21726199]

Brittain T, Skommer J. Does a redox cycle provide a mechanism for setting the capacity of neuroglobin to protect cells from apoptosis? IUBMB Life. 2012; 64:419–22. [PubMed: 22362590]

Brunori M, Giuffre A, Nienhaus K, et al. Neuroglobin, nitric oxide, and oxygen: functional pathways and conformational changes. Proc Natl Acad Sci U S A. 2005; 102:8483–8. [PubMed: 15932948]

Burmester T, Hankeln T. What is the function of neuroglobin? J Exp Biol. 2009; 212:1423–8. [PubMed: 19411534]

Burmester T, Weich B, Reinhardt S, et al. A vertebrate globin expressed in the brain. Nature. 2000; 407:520–3. [PubMed: 11029004]

Chan JK, Charrier JG, Kodani SD, et al. Combustion-derived flame generated ultrafine soot generates reactive oxygen species and activates Nrf2 antioxidants differently in neonatal and adult rat lungs. Part Fibre Toxicol. 2013; 10:34. [PubMed: 23902943]

Chen L, Lee HM, Greeley GH Jr, et al. Accumulation of oxidatively generated DNA damage in the brain: a mechanism of neurotoxicity. Free Radic Biol Med. 2007; 42:385–93. [PubMed: 17210451]

Cui J, Liu PK. Neuronal NOS inhibitor that reduces oxidative DNA lesions and neuronal sensitivity increases the expression of intact c-fos transcripts after brain injury. J Biomed Sci. 2001; 8:336–41. [PubMed: 11455196]

Dranka BP, Benavides GA, Diers AR, et al. Assessing bioenergetic function in response to oxidative stress by metabolic profiling. Free Radic Biol Med. 2011; 51:1621–35. [PubMed: 21872656]

Droge J, Pande A, Englander EW, et al. Comparative genomics of neuroglobin reveals its early origins. PLoS One. 2012; 7:e47972. [PubMed: 23133533]

Edye ME, Lopez-Castejon G, Allan SM, et al. Acidosis drives damage-associated molecular pattern (DAMP)-induced interleukin-1 secretion via a caspase-1-independent pathway. J Biol Chem. 2013; 288:30485–94. [PubMed: 24022484]

Fago A, Mathews AJ, Moens L, et al. The reaction of neuroglobin with potential redox protein partners cytochrome b5 and cytochrome c. FEBS Lett. 2006; 580:4884–8. [PubMed: 16914148]

Fiocchetti M, De Marinis E, Ascenzi P, et al. Neuroglobin and neuronal cell survival. Biochim Biophys Acta. 2013; 1834:1744–9. [PubMed: 23357651]

Fisar Z, Hroudova J, Raboch J. Inhibition of monoamine oxidase activity by antidepressants and mood stabilizers. Neuro Endocrinol Lett. 2010; 31:645–56. [PubMed: 21200377]

Flynn JM, Choi SW, Day NU, et al. Impaired spare respiratory capacity in cortical synaptosomes from Sod2 null mice. Free Radic Biol Med. 2011; 50:866–73. [PubMed: 21215798]

Fordel E, Thijs L, Moens L, et al. Neuroglobin and cytoglobin expression in mice. Evidence for a correlation with reactive oxygen species scavenging. FEBS J. 2007; 274:1312–7. [PubMed: 17286577]

Gerencser AA, Neilson A, Choi SW, et al. Quantitative microplate-based respirometry with correction for oxygen diffusion. Anal Chem. 2009; 81:6868–78. [PubMed: 19555051]

Ghosh N, Ghosh R, Mandal SC. Antioxidant protection: A promising therapeutic intervention in neurodegenerative disease. Free Radic Res. 2011; 45:888–905. [PubMed: 21615270]

Hankeln T, Wystub S, Laufs T, et al. The cellular and subcellular localization of neuroglobin and cytoglobin -- a clue to their function? IUBMB Life. 2004; 56:671–9. [PubMed: 15804831]

Hartzell GE. Overview of combustion toxicology. Toxicology. 1996; 115:7–23. [PubMed: 9016738]

Herold S, Fago A, Weber RE, et al. Reactivity studies of the Fe(III) and Fe(II)NO forms of human neuroglobin reveal a potential role against oxidative stress. J Biol Chem. 2004; 279:22841–7. [PubMed: 15020597]

Hroudova J, Fisar Z. In vitro inhibition of mitochondrial respiratory rate by antidepressants. Toxicol Lett. 2012; 213:345–52. [PubMed: 22842584]

Hundahl CA, Allen GC, Hannibal J, et al. Anatomical characterization of cytoglobin and neuroglobin mRNA and protein expression in the mouse brain. Brain Res. 2010; 1331:58–73. [PubMed: 20331985]

Hundahl CA, Fahrenkrug J, Hay-Schmidt A, et al. Circadian behaviour in neuroglobin deficient mice. PLoS One. 2012; 7:e34462. [PubMed: 22496809]

Hundahl CA, Kelsen J, Dewilde S, et al. Neuroglobin in the rat brain (II): co-localisation with neurotransmitters. Neuroendocrinology. 2008; 88:183–98. [PubMed: 18509243]

Hundahl CA, Luuk H, Ilmjarv S, et al. Neuroglobin-deficiency exacerbates Hif1A and c-FOS response, but does not affect neuronal survival during severe hypoxia in vivo. PLoS One. 2011; 6:e28160. [PubMed: 22164238]

Khan AA, Wang Y, Sun Y, et al. Neuroglobin-overexpressing transgenic mice are resistant to cerebral and myocardial ischemia. Proc Natl Acad Sci U S A. 2006; 103:17944–8. [PubMed: 17098866]

Kiger L, Tilleman L, Geuens E, et al. Electron transfer function versus oxygen delivery: a comparative study for several hexacoordinated globins across the animal kingdom. PLoS One. 2011; 6:e20478. [PubMed: 21674044]

Kovacs KJ. Measurement of immediate-early gene activation- c-fos and beyond. J Neuroendocrinol. 2008; 20:665–72. [PubMed: 18601687]

Lechauve C, Augustin S, Cwerman-Thibault H, et al. Neuroglobin involvement in respiratory chain function and retinal ganglion cell integrity. Biochim Biophys Acta. 2012; 1823:2261–73. [PubMed: 23036890]

Lee HM, Greeley GH, Herndon DN, et al. A rat model of smoke inhalation injury: influence of combustion smoke on gene expression in the brain. Toxicol Appl Pharmacol. 2005; 208:255–65. [PubMed: 15893353]

Lee HM, Greeley GH Jr, Englander EW. Transgenic overexpression of neuroglobin attenuates formation of smoke-inhalation-induced oxidative DNA damage, in vivo, in the mouse brain. Free Radic Biol Med. 2011; 51:2281–7. [PubMed: 22001746]

Lee HM, Hallberg LM, Greeley GH Jr, et al. Differential inhibition of mitochondrial respiratory complexes by inhalation of combustion smoke and carbon monoxide, in vivo, in the rat brain. Inhal Toxicol. 2010; 22:770–7. [PubMed: 20429857]

Lee HM, Reed J, Greeley GH Jr, et al. Impaired mitochondrial respiration and protein nitration in the rat hippocampus after acute inhalation of combustion smoke. Toxicol Appl Pharmacol. 2009; 235:208–15. [PubMed: 19133281]

Li W, Wu Y, Ren C, et al. The activity of recombinant human neuroglobin as an antioxidant and free radical scavenger. Proteins. 2011; 79:115–25. [PubMed: 20938977]

Loane C, Pilinis C, Lekkas TD, et al. Ambient particulate matter and its potential neurological consequences. Rev Neurosci. 2013; 24:323–35. [PubMed: 23612538]

Raychaudhuri S, Skommer J, Henty K, et al. Neuroglobin protects nerve cells from apoptosis by inhibiting the intrinsic pathway of cell death. Apoptosis. 2010; 15:401–11. [PubMed: 20091232]

Renner K, Amberger A, Konwalinka G, et al. Changes of mitochondrial respiration, mitochondrial content and cell size after induction of apoptosis in leukemia cells. Biochim Biophys Acta. 2003; 1642:115–23. [PubMed: 12972300]

Rogers GW, Brand MD, Petrosyan S, et al. High throughput microplate respiratory measurements using minimal quantities of isolated mitochondria. PLoS One. 2011; 6:e21746. [PubMed: 21799747]

Ross JM, Oberg J, Brene S, et al. High brain lactate is a hallmark of aging and caused by a shift in the lactate dehydrogenase A/B ratio. Proc Natl Acad Sci U S A. 2010; 107:20087–92. [PubMed: 21041631]

Rossi J 3rd, Ritchie GD, Macys DA, et al. An overview of the development, validation, and application of neurobehavioral and neuromolecular toxicity assessment batteries: potential applications to combustion toxicology. Toxicology. 1996; 115:107–17. [PubMed: 9016744]

Schmittgen TD, Livak KJ. Analyzing real-time PCR data by the comparative C(T) method. Nat Protoc. 2008; 3:1101–8. [PubMed: 18546601]

Shimokawa N, Dikic I, Sugama S, et al. Molecular responses to acidosis of central chemosensitive neurons in brain. Cell Signal. 2005; 17:799–808. [PubMed: 15763422]

Sims NR, Anderson MF. Isolation of mitochondria from rat brain using Percoll density gradient centrifugation. Nat Protoc. 2008; 3:1228–39. [PubMed: 18600228]

Sims NR, Blass JP. Expression of classical mitochondrial respiratory responses in homogenates of rat forebrain. J Neurochem. 1986; 47:496–505. [PubMed: 3734792]

Singh S, Englander EW. Nuclear depletion of apurinic/apyrimidinic endonuclease 1 (Ape1/Ref-1) is an indicator of energy disruption in neurons. Free Radic Biol Med. 2012; 53:1782–90. [PubMed: 22841870]

Singh S, Zhuo M, Gorgun FM, et al. Overexpressed neuroglobin raises threshold for nitric oxide-induced impairment of mitochondrial respiratory activities and stress signaling in primary cortical neurons. Nitric Oxide. 2013; 32:21–8. [PubMed: 23587847]

Stefanidou M, Athanaselis S, Spiliopoulou C. Health impacts of fire smoke inhalation. Inhal Toxicol. 2008; 20:761–6. [PubMed: 18569098]

Sun Y, Jin K, Peel A, et al. Neuroglobin protects the brain from experimental stroke in vivo. Proc Natl Acad Sci U S A. 2003; 100:3497–500. [PubMed: 12621155]

Tiedke J, Cubuk C, Burmester T. Environmental acidification triggers oxidative stress and enhances globin expression in zebrafish gills. Biochem Biophys Res Commun. 2013; 441:624–9. [PubMed: 24177009]

Wallace DC. A mitochondrial bioenergetic etiology of disease. J Clin Invest. 2013; 123:1405–12. [PubMed: 23543062]

Watanabe S, Takahashi N, Uchida H, et al. Human neuroglobin functions as an oxidative stress-responsive sensor for neuroprotection. J Biol Chem. 2012; 287:30128–38. [PubMed: 22787149]

Watanabe S, Wakasugi K. Neuroprotective function of human neuroglobin is correlated with its guanine nucleotide dissociation inhibitor activity. Biochem Biophys Res Commun. 2008; 369:695–700. [PubMed: 18302932]

Yu Z, Poppe JL, Wang X. Mitochondrial mechanisms of neuroglobin's neuroprotection. Oxid Med Cell Longev. 2013; 2013:756989. [PubMed: 23634236]

Yu Z, Xu J, Liu N, et al. Mitochondrial distribution of neuroglobin and its response to oxygen-glucose deprivation in primary-cultured mouse cortical neurons. Neuroscience. 2012; 218:235–42. [PubMed: 22659017]

Zou YY, Kan EM, Cao Q, et al. Combustion smoke-induced inflammation in the cerebellum and hippocampus of adult rats. Neuropathol Appl Neurobiol. 2013; 39:531–52. [PubMed: 23106634]

Zou YY, Lu J, Poon DJ, et al. Combustion smoke exposure induces up-regulated expression of vascular endothelial growth factor, aquaporin 4, nitric oxide synthases and vascular permeability in the retina of adult rats. Neuroscience. 2009; 160:698–709. [PubMed: 19285541]

Zsurka G, Kunz WS. Mitochondrial involvement in neurodegenerative diseases. IUBMB Life. 2013; 65:263–72. [PubMed: 23341346]

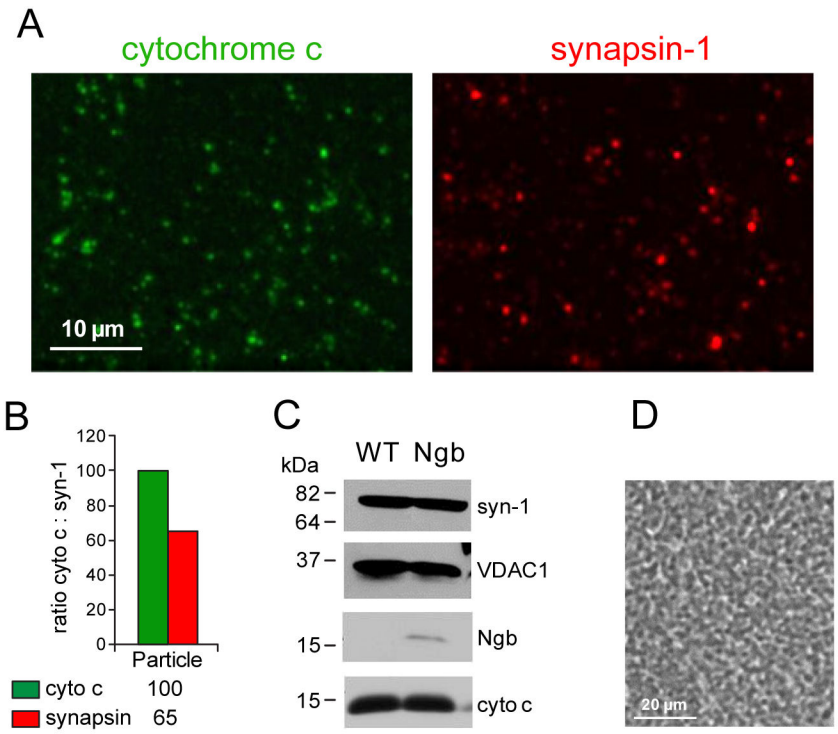

Fig 1. Examination of crude mitochondrial preparations from the mouse cortex

(A) Representative immunofluorescent images of mitochondrial spreads (wild type) reacted with cytochrome c (green) and synapsin 1 (red) antibodies (40X magnification) are shown. (B) Graphical representation of ImageJ quantification of cytochrome c (green) and synapsin (red) positive particles. (C) Western blotting analysis of crude mitochondrial preparations probed for the mitochondrial outer membrane, voltage dependent anion channel protein 1 (VDAC1) and the inter-membrane space cytochrome c protein. Detection of the synaptosomal protein, synapsin 1, confirmed the presence of synaptosomal component in cortical mitochondria preparations. Neuroglobin was detected in preparations from Ngb-tg but not the wild type cortex. (D) Representative contrast phase image of uniformly distributed crude mitochondrial preparations in XF24 plates (6 µg/well) loaded for oxygen consumption analyses (20X magnification).

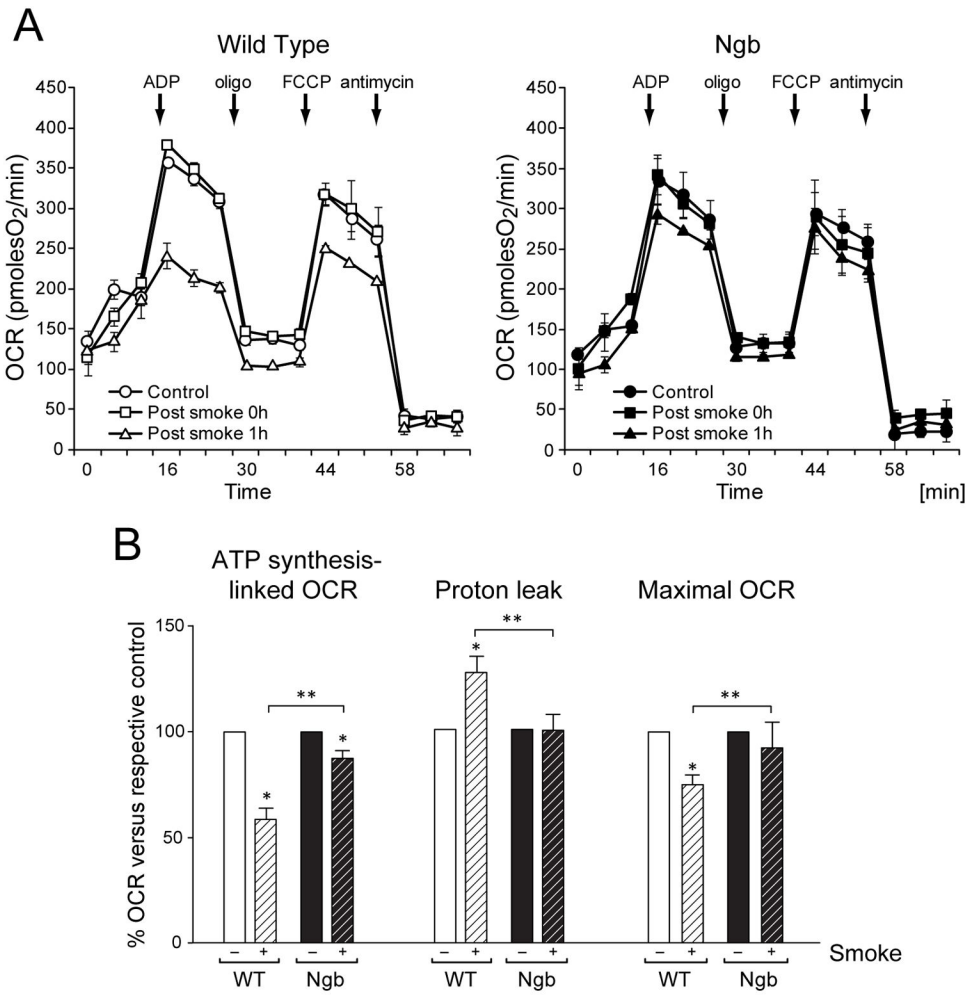

Fig 2. Differential effects of combustion smoke on respiratory profiles of wild type and Ngb-tg cortical mitochondria

Mitochondrial respiration was analyzed using the Seahorse XF24 flux analyzer. Mitochondria isolated from sham-controls and post smoke wild type and Ngb-tg mice were placed in the XF24 plates. (A) Respiratory profiles are shown for the wild type [open symbols, left panel] and Ngb-tg [solid symbols, right panel] mitochondria: sham-controls and mice at 0 and 1-hour post smoke exposure were analyzed. Sequential, in port additions of ADP and mitochondrial effectors are indicated by downward arrows and their timing is marked on the x-axis (minutes). OCR values demarcated on the y-axis measure the relative OCR changes. ATP synthesis-linked OCR measured in sham-controls (circles) was significantly reduced at 1 hour [triangles], but not immediately (0 hour) after smoke exposure (squares). A lesser reduction was measured at the 1-hour recovery time (solid triangles) in Ngb-tg mitochondria when compared to wild type (solid circles). (B) The extent of changes for the 1-hour post smoke recovery time versus sham-controls was calculated for WT [open bars] and Ngb-tg [solid bars] for the different segments of respiratory profiles and graphically presented in panel B: Relative changes in ATP synthesis linked OCR revealed a ~40% reduction for the WT (open) versus an ~15% reduction for Ngb-tg (solid). Measurements of OCR feeding the proton leak (after injection of oligomycin) showed a 26%

increase for the WT and no increase in proton leakage for Ngb-tg after smoke. Following smoke exposure, relative FCCP-induced OCR was ~25% lower compared to sham control for the WT and ~10% lower in the case of Ngb-tg (statistically not significant). Relative changes are presented as means ± SEM (n=6). * designates different from each respective sham-control and ** different from WT for a given treatment; $p<0.05$ significance.

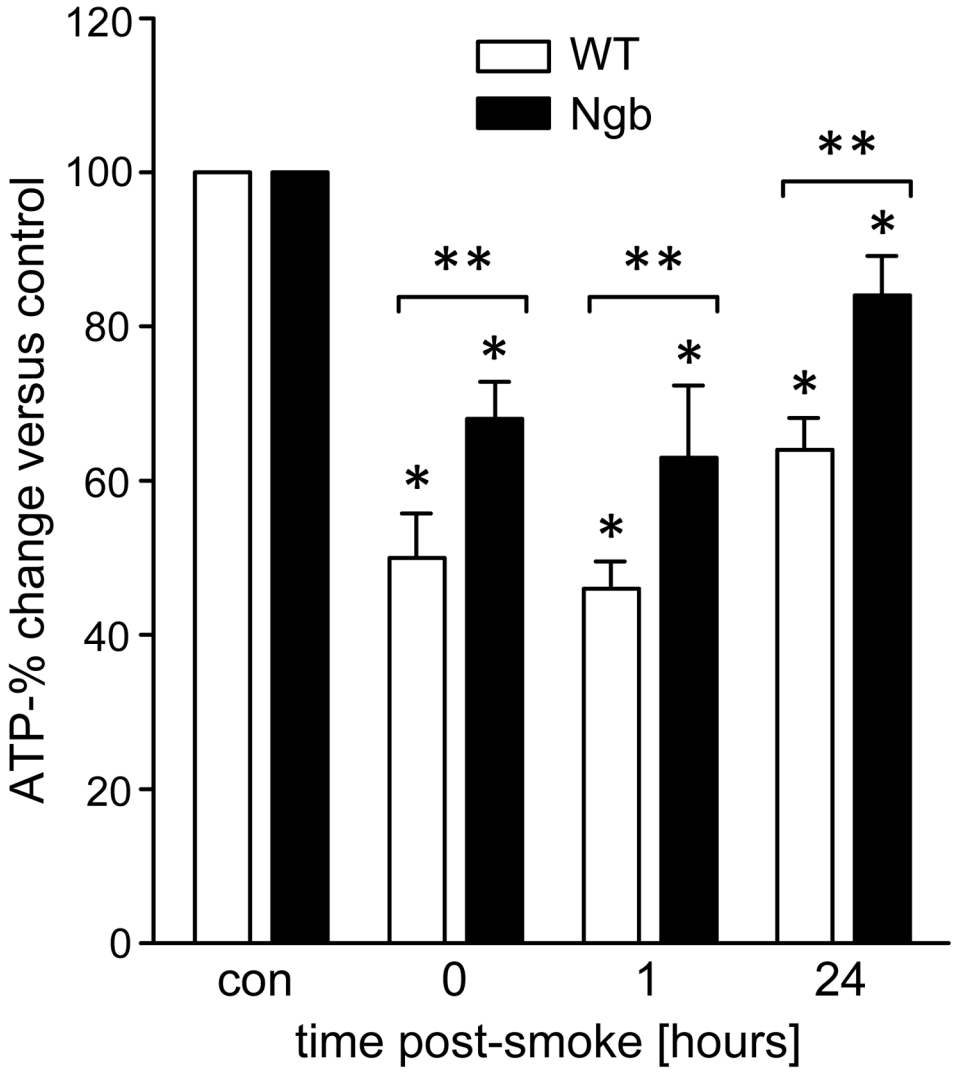

Fig 3. Mitochondrial ATP content is differentially affected by smoke in the wild type and Ngb-tg brain

Mitochondrial ATP content was determined using the ATP Bioluminescence Assay and normalized to protein amount. ATP content was reduced by exposure to smoke: approximately 50% and 35% reductions were observed at the 0- and 1-hour and ~35% and 15% at 24-hours post smoke in the wild type and Nb-tg mitochondria, respectively. Values are presented as means ± SEM (n=4); * designates different from each respective sham-control and **designates different from WT for a given treatment; $p<0.05$.

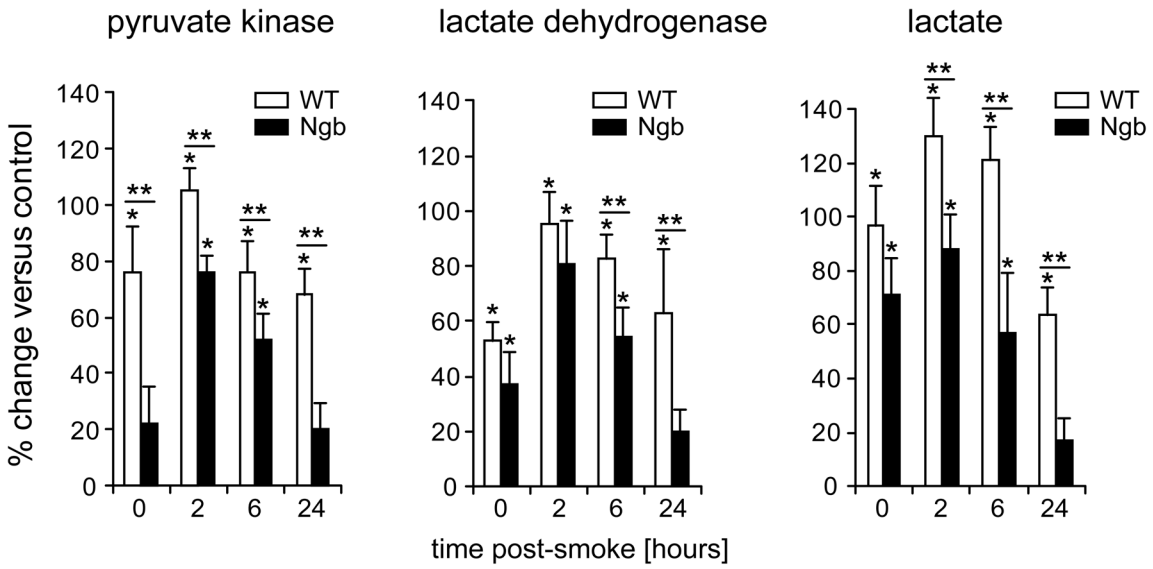

Fig 4. Acute smoke inhalation differentially modulates cytosolic energy metabolism in the wild type and Ngb-tg brain

Measurements of changes in cytosolic pyruvate kinase (PK), lactate dehydrogenase (LDH) and lactic acid levels in the wild type and Ngb-tg brains harvested at 0, 2, 6 and 24 hours after exposures to smoke are shown; levels were elevated at all time points. In the wild type but not Ngb-tg brain, significant increases persisted also at the 24-hour recovery. Values are presented as percent of control and expressed as means ± SEM (n=4). * indicates different from the respective control; ** indicates different from wild type for a given treatment; $p < 0.05$.

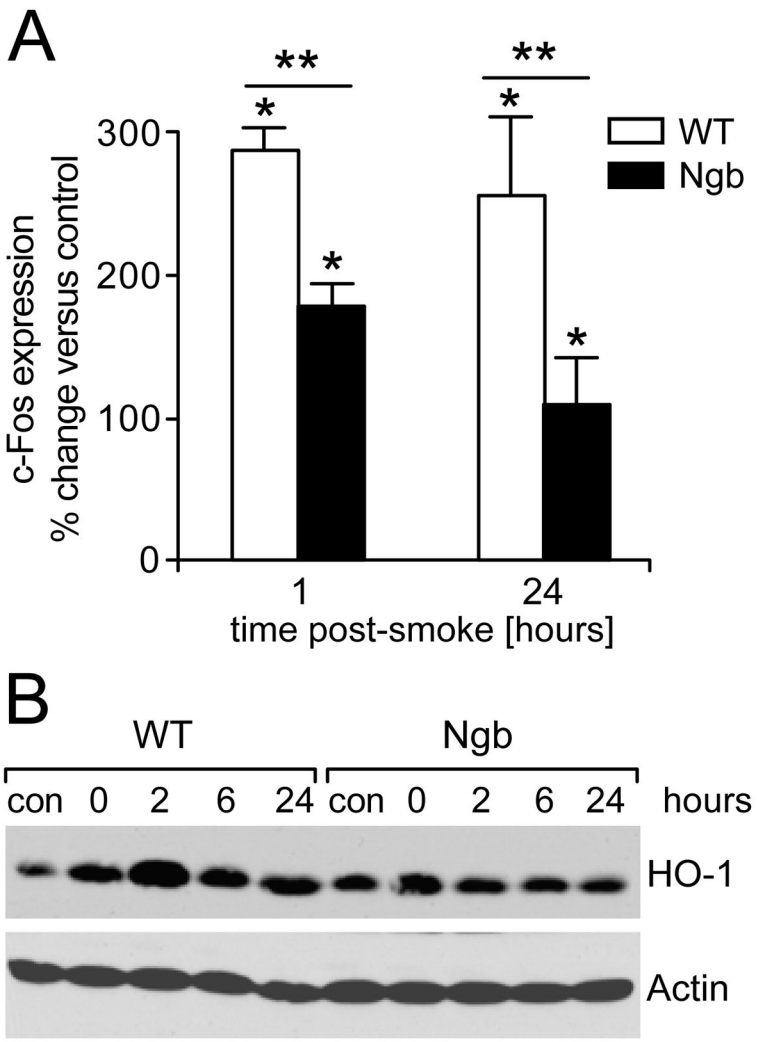

Fig 5. c-Fos and heme oxygenase-1 are differentially induced in the wild type and Ngb-tg cortex after smoke inhalation

(A) c-Fos gene expression is elevated following smoke inhalation. Relative changes in c-Fos mRNA levels measured by RT-qPCR are presented as bar graphs (means ± SEM; n=5). * indicates different from respective control and ** indicates different from wild type for a given treatment; $p < 0.05$. (B) Representative image of Western blotting analysis of heme oxygenase-1 (HO-1) levels is shown for wild type and Ngb-tg cortices at 0, 2, 6 and 24 hours recovery after smoke. Western detection of actin levels serves as loading control.